Proceedings Paper:
Sonnenwald, F. and Guymer, I. (2024) Reach unified channel characteristics for the transverse advection-dispersion equation. In: Kalinowska, M.B., Mrokowska, M.M. and Rowiński, P.M., (eds.) Advances in Hydraulic Research: 40th International School of Hydraulics. 40th International School of Hydraulics (ISH 2023), 23-26 May 2023, Kąty Rybackie, Poland. GeoPlanet: Earth and Planetary Sciences. Springer Cham, pp. 363-374. ISBN: 9783031560927. ISSN: 2190-5193. EISSN: 2190-5207.

https://doi.org/10.1007/978-3-031-56093-4_29

Reach unified channel characteristics for the transverse advection-dispersion equation

Fred Sonnenwald and Ian Guymer

Abstract Transverse dispersion is of interest in natural watercourses, especially near outfalls. The application of simple analytical solutions to the transverse advection-dispersion equation in these scenarios, however, is challenging due to variations in channel characteristics. Thus, a new method has been developed for averaging reach characteristics to account for longitudinal variability when using analytical solutions to the advection-dispersion equation by combining travel time and length weighting. The new 'reach unification' approach incorporates the characteristics (such as velocity, width, or dispersion coefficient) of each different sub-reach into to the equivalent single reach values needed to make a direct downstream prediction. To demonstrate reach unification, synthetic concentration profiles from a continuous injection into a simplified rectangular channel with three sub-reaches of varying velocity, depth, and friction, have been generated using finite difference modelling. The characteristics of these sub-reaches when combined with reach unification made perfect downstream analytical predictions, confirming the approach. The use of the streamtube model to represent changes in channel width is investigated. It is also shown that reach unification is of significant benefit to the inverse problem, analysing recorded concentration profiles to estimate the dispersion coefficient and relating it to reach characteristics.

F. Sonnenwald · I. Guymer
Department of Civil and Structural Engineering, The University of Sheffield, Mappin St., Sheffield, S1 3JD, UK.
e-mail: f.sonnenwald@sheffield.ac.uk

I. Guymer
e-mail: i.guymer@sheffield.ac.uk

1 Introduction

Mixing, the description of the transport and spread of solutes, can be described by the three-dimensional Advection-Dispersion Equation (ADE):

$$\frac{\partial c}{\partial t} + u\frac{\partial c}{\partial x} + v\frac{\partial c}{\partial y} + w\frac{\partial c}{\partial z} = D_x\frac{\partial^2 c}{\partial x^2} + D_y\frac{\partial^2 c}{\partial y^2} + D_z\frac{\partial^2 c}{\partial z^2} \tag{1}$$

where c is concentration, t is time, u, v, and w are the velocity components in the longitudinal (x), transverse (y), and vertical (z) directions, and D_x, D_y, and D_z are the dispersion coefficients in those same directions (Fischer et al, 1979). In simple systems, such as pipes, this is often simplified into a one-dimensional (1D) equation in the direction of flow, e.g., Taylor (1954). While this simplification is also often made in natural watercourses over long distances, local mixing conditions tend to be sufficiently complex to warrant a more detailed description over shorter distances. The mixing of a point pollution source can generally be divided into three regions: the near-field, where primarily vertical mixing is of interest, the mid-field, where primarily transverse mixing is of interest, and the far-field, where primarily longitudinal mixing is of interest (Rutherford, 1994).

This study focuses on the mid-field mixing region, i.e., transverse mixing. The mid-field is primarily of interest shortly downstream from outfalls, before complete cross-sectional mixing has occurred. Descriptions of mixing are needed in this region to help ensure nominally acceptable levels of outfall pollutants become sufficiently dilute to not cause undue damage to the watercourse (Yotsukura and Cobb, 1972). This can occur both in the form of biochemical (Riechel et al, 2016) or thermal pollution (Kalinowska and Rowiński, 2012). In the far-field, the rate of transverse dispersion affects the rate of longitudinal dispersion (Fischer et al, 1979).

The complexity of describing mixing in the mid-field, and in watercourses in general, is derived from not only changes in channel cross-section, but also due to associated changes in roughness and velocities. These can be considered together within the two-dimensional (2D) depth-averaged ADE:

$$h(y)u(y)\frac{\partial c(x,y)}{\partial x} = \frac{\partial}{\partial y}\left[h(y)D_y(y)\frac{\partial c(x,y)}{\partial y}\right] \tag{2}$$

where h is depth (West et al, 2021). This approach has been used to describe complex transverse mixing conditions. West et al (2021) created a Finite Difference Model (FDM) of dispersion in the shear layer adjacent to bankside vegetation using Eq. 2. This model was used to identify the transverse variation of D_y by fitting to concentration data collected using a laser-induced fluorescence camera system in partially vegetated channel flow.

While detailed mixing descriptions of complex flow situations can be provided by numerical modelling or advanced instrumentation, in practice results are often obtained through manual sampling at or moving the same instrument(s) to multiple measurement locations (e.g., Boxall and Guymer, 2003). Such methods are practical

and in line with that are simpler analytical solutions to the ADE (Rutherford, 1994). For a continuous injection, Eq. 1 simplifies to the 1D transverse ADE:

$$u\frac{\partial c}{\partial x} = D_y\frac{\partial^2 c}{\partial y^2} \tag{3}$$

One analytical solution to this is given by the 1D transverse ADE routing solution:

$$c(x_2,y) = \int_{\lambda=-\infty}^{\infty} \frac{c(x_1,\lambda)}{\sqrt{4\pi D_y \bar{t}}} \exp\left[-\frac{(\lambda - y - V\bar{t})^2}{4D_y\bar{t}}\right] \mathrm{d}\lambda \tag{4}$$

where x_1 and x_2 are upstream and downstream measurement locations respectively, $\bar{t} = (x_2 - x_1)/U$ is travel time, and U and V (0 in theory) are mean streamwise and transverse velocities (Stovin et al, 2022). Eq. 4 applies to uniform conditions only.

Another simplified approach for cross-sectionally varying velocity and bathymetry is given by Yotsukura and Sayre (1976). The cumulative discharge or 'streamtube' model, accounts for changes in channel cross-section by transforming transverse distance coordinates to equivalent increases in cumulative discharge q, equalling 0 at the left bank and total discharge Q at the right bank (Rutherford, 1994). Thus, a wide and shallow flow may be equated to a narrow deep flow by 'stretching' or 'squeezing' the flow field cross-section to a uniform depth, straightening streamtubes. The solution to a continuous injection at q_0 is given by

$$c(x,q) = \frac{m}{\sqrt{4\pi D_q x}} \exp\left(-\frac{(q-q_0)^2}{4D_q x}\right) \tag{5}$$

where m is injection flow rate,

$$D_q = \psi H^2 U D_y \tag{6}$$

is the transformed transverse dispersion in streamtube coordinates,

$$\psi = \frac{1}{B}\int_{y=0}^{B} \left(\frac{h}{H}\right)^2 \frac{u}{U}\mathrm{d}y \tag{7}$$

is a shape factor, B is channel breadth, and H is mean depth (Rutherford, 1994). In a rectangular channel with uniform velocity, the shape factor will take a value of 1. A reflecting boundary condition at the channel bank may be achieved using the method of images and an equivalent routing solution of Eq. 5 to Eq. 4 can be derived.

Although the streamtube model may account for changes in cross-section, it does not account for other longitudinal changes, such as changes in roughness or other characteristics that may influence transverse mixing. Somlyódy (1982) further refines the streamtube model, presenting a "mass streamline" line model that better accounts for longitudinal variations, but at the cost of significantly increased model complexity. Alternatively, Rutherford (1994) suggests that, whether applying Eqs. 4

or 5, longitudinal variations in transverse dispersion may be accounted for using distance, or length, weighted averaging.

To investigate averaging channel characteristics for longitudinal dispersion, Sonnenwald et al (2023) substituted the 1D longitudinal ADE routing solution into itself and found the single D_x, U, and $\bar{t}$ needed to be equivalent to two or more routings carried out in series. This combining of multiple routings into a single routing, or multiple sub-reaches into a single reach, led to the 'reach unification' approach. Taking velocity as travel time weighted ($U = \sum_{i=1}^{N} U_i \bar{t}_i / \sum_{i=1}^{N} \bar{t}_i$), D_x was found to be:

$$D_x = \frac{\left(\sum_{i=1}^{N} U_i \bar{t}_i\right)^2 \sum_{i=1}^{N} \left(D_{x,i} \bar{t}_i \prod_{j=1, j\neq i}^{N} U_j^2\right)}{\left(\prod_{i=1}^{N} U_i^2\right) \left(\sum_{i=1}^{N} \bar{t}_i^3\right)} \tag{8}$$

and by assuming $D_x = \alpha U$, the relationship for all other characteristics α (depth, etc.) was found to be:

$$\alpha = U \frac{\sum_{i=1}^{N} \alpha_i \bar{t}_i / U_i}{\sum_{i=1}^{N} \bar{t}_i} \tag{9}$$

where i and j are the i^{th} and j^{th} routing, and N is the number of routings or sub-reaches.

Equations 8-9 show that different averaging treatments are required for different components of the 1D longitudinal ADE. This result calls into question the length weighted averaging proposed by Rutherford (1994) for transverse dispersion. Therefore, this study aims to provide an appropriate method for averaging reach characteristics to simplify the application of the ADE for transverse mixing.

2 Methodology

Herein the new reach unification averaging approach is derived for the transverse ADE and the creation of synthetic data for validation using numerical modelling data is explained.

2.1 Transverse reach unified averaging derivation

A single reach may be made up of many sub-reaches, e.g., Fig. 1. If an injection is made upstream of sub-reach A at location 0, the dye passes through sub-reaches A, B, and C. If monitoring of transverse concentration distributions is conducted at the end of each sub-reach at locations a, b, and c, then the transverse dispersion coefficient in sub-reach A, $D_{y,A}$, can be calculated from the increase in transverse variance of the recorded concentration profile between 0 and a, $D_{y,B}$ as the increase in transverse variance between b and a, etc. This approach to finding dispersion coefficient is referred to as the method of moments (Rutherford, 1994). A downstream predic-

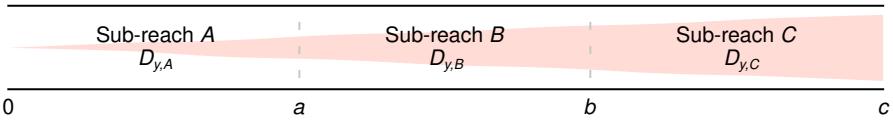

Fig. 1 Example reach.

tion at a may be made with Eq. 4 using the initial injection, $D_{y,A}$, and the travel time. This prediction can be substituted as the upstream concentration distribution in Eq. 4 with $D_{y,B}$ and the travel time to make a prediction at b, etc. A prediction at c would therefore consist of some combination of the transverse dispersion coefficients $D_{y,A}$, $D_{y,B}$, and $D_{y,C}$.

Although Sonnenwald et al (2023) conceptualised this approach by substituting the routing solution into itself, SG Wallis (2022 personal communication) suggested a simpler derivation should be possible by directly manipulating the method of moments variances. This has been done here for the transverse dispersion coefficient. The method of moments solution to obtaining the transverse dispersion coefficient is:

$$D_y = \frac{U}{2}\frac{\left(\sigma_2^2 - \sigma_1^2\right)}{\left(x_2 - x_1\right)} \tag{10}$$

where σ_1^2 and σ_2^2 are the spatial variances of the transverse concentration profile at locations x_1 and x_2 (Rutherford, 1994). (For the example reach in Fig. 1, using σ_a^2, σ_b^2 , a, and b in Eq. 10 would give $D_{y,B}$.)

Re-arranging and simplifying Eq. 10, downstream variance can be predicted as a function of the upstream variance and the dispersion coefficient:

$$\sigma_2^2 = 2\bar{t}D_y + \sigma_1^2 \tag{11}$$

Considering two sub-reaches and substituting the downstream variance as the upstream variance for the downstream sub-reach:

$$\sigma_3^2 = 2\bar{t}_2 D_{y2} + 2\bar{t}_1 D_{y1} + \sigma_1^2 \tag{12}$$

This can be re-arranged and substituted into Eq. 10 to find D_y for the reach. Simplified and generalised, this gives the reach unified transverse dispersion coefficient as:

$$D_y = \frac{\sum_{i=1}^{N} D_{y,i}\bar{t}_i}{\sum_{i=1}^{N} \bar{t}_i} \tag{13}$$

Eq. 13 shows that for the transverse ADE, the transverse dispersion coefficient is travel time weighted, as opposed to length weighted, as suggested by Rutherford (1994, Sect. 3.4.4.2). By substituting in $D_y = \alpha U$, i.e., dispersion as a function of some parameter multiplied by velocity (Taylor, 1954; Fischer et al, 1979), it follows that channel characteristics should be length weighted:

$$\alpha = \frac{\sum_{i=1}^{N} \alpha_i \Delta x_i}{\sum_{i=1}^{N} \Delta x_i} \tag{14}$$

where Δx_i is the sub-reach length (i.e., $x_i - x_{i-1}$). If a property does not scale linearly with D_y, then a substitution for α should be made and Eq. 14 updated accordingly. For example, in the case of $D_y = \beta^2 U$ then β^2 should be substituted for α and β_i^2 for α_i. Note that the transverse ADE reach unified characteristics are calculated differently to the longitudinal ADE.

2.2 Synthetic concentration data

The West et al (2021) finite difference model of the 2D depth-averaged ADE has been used to generate synthetic concentration data for testing reach unification. The FDM model uses a central scheme for dispersion and an upwind scheme for advection. It consists of a series of equations forming a tri-diagonal matrix, which is solved using the 'double sweep' algorithm. Transverse boundary conditions are reflective. West et al (2021) validated the FDM against analytical solutions to the ADE.

For validating reach unification, the FDM was used to generate synthetic concentration data for 100 rectangular channels consisting of three sub-reaches. For the example reach, channel characteristics are given in Table 1 with a uniform channel width of 6 m and flow rate of 3 m^3s^{-1}. Sub-reach transverse dispersion coefficient was taken as:

$$D_y = 0.13U\sqrt{f/8} \tag{15}$$

where f is a friction factor (after Boxall and Guymer, 2003). A mid-channel injection was used.

The channel characteristics of the remaining 99 channels were randomised. Sub-reach length was picked between 5 and 500 m, U between 0.01 and 1 ms^{-1}, H between 0.5 and 50 m (ensuring continuity with $Q = 5$ m^3s^{-1}), and f between 0.001 and 0.5. The width of the random channels was manipulated to simulate an infinitely far away transverse boundary in order to make direct comparisons to Eq. 4 without the need for the method of images.

Table 1 Example sub-reach characteristics and reach unified (+) characteristics

Sub-reach	Length (m)	U (ms^{-1})	$\bar{t}$ (s)	H (m)	f	D_y (m^2s^{-1})
A	5	0.500	10	1	0.01	2.3×10^{-3}
B	10	0.250	40	2	0.05	2.6×10^{-3}
C	15	0.125	120	4	0.10	1.8×10^{-3}
$A+B$	15	0.300	50	1.67	0.03	2.5×10^{-3}
$A+B+C$	30	0.177	170	2.83	0.06	2.0×10^{-3}

The concentration profiles generated by the FDM were treated as the 'known' result (e.g., a laboratory measurement) and compared to predictions made using Eq. 4 and the reach unified D_y. This comparison was made using the R_t^2 correlation measure:

$$R_t^2 = 1 - \frac{\sum_{i=1}^{n}(\hat{c}_i - c_i)^2}{\sum_{i=1}^{n} c_i^2} \tag{16}$$

where $\hat{c}$ is predicted concentration and n is the number of points in the concentration profile. An R_t^2 of 1 indicates perfect agreement and $R_t^2 \leq 0$ indicates no agreement (Young et al, 1980).

3 Results and discussion

Figure 2 shows the finite difference model concentration profiles for the channel described in Table 1 compared to the concentration profiles calculated directly using the routing solution (Eq. 4) and the reach unified D_y. The R_t^2 values comparing the FDM and predicted concentrations were both 1.000. If D_y were to be calculated using a length weighted average, then concentrations at b would be very slightly over-predicted, and at c slightly under-predicted.

Figure 3 compares the goodness-of-fit between predicted concentration profiles made using reach unified D_y to those made using length weighted D_y for the 99 random channels. As suggested by the example reach results, the difference in the predictions is small in many cases. Goodness-of-fit when using the length weighted dispersion coefficient decreases with increased travel time, i.e., more time in the flow.

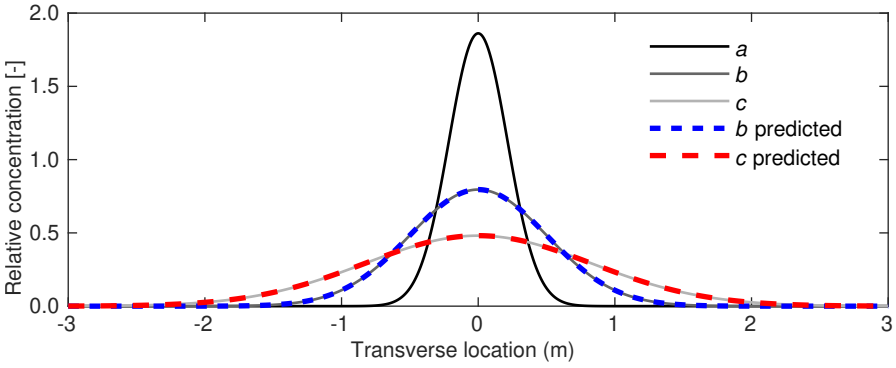

Fig. 2 Example reach concentration profiles (calculated using the FDM, solid lines) and reach unified predictions (calculated using Eq. 4, dashed lines).

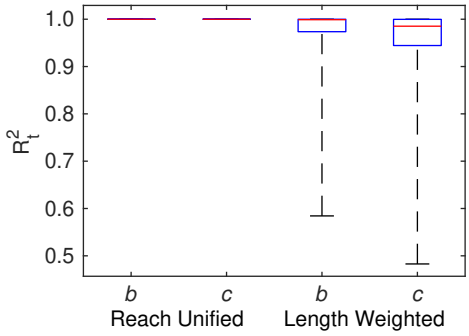

Fig. 3 A box plot of R_t^2 values comparing predictions made using reach unified and length weighted averaging of D_y for random channels at sections *b* and *c*. Middle line indicates median, box indicates interquartile range, and whiskers indicate range.

3.1 Accounting for changes in width

Reach unified values account for changes in channel properties, such as depth, velocity, etc. This technically includes the effects of changes in width but does not address the spreading of a solute caused by changes in bathymetry. If a channel increases in width, becoming more shallow, the measured depth-averaged concentration profile would increase in width. While this could be ignored, and Eq. 4 applied regardless, D_y at that point would no longer be linked directly to flow conditions. Instead, this bulk spreading can be taken into account using the streamtube model (Rutherford, 1994).

Considering the general form of Eq. 5, it stands to reason that reach unification may have some application to the streamtube model to allow for a direct prediction downstream of several different cross-sections. In Eq. 5, D_q takes the units m^5s^{-2}, which is multiplied by the distance downstream. Following a similar reach unification analysis as presented in Sect. 2.1 for D_q, length weighted averaging should be applied:

$$D_q = \frac{\sum_{i=1}^{N} D_{q,i} \Delta x_i}{\sum_{i=1}^{N} \Delta x_i} \tag{17}$$

Using the FDM modified to adjust concentrations between sub-reaches using the streamtube principle and investigating a channel of increasing width confirms this result. The FDM also shows that reach unified D_q cannot be calculated directly from reach unified characteristics and Eq. 6 and instead D_q for each sub-reach must be calculated before reach unification.

The appearance of length weighted averaging for D_q in Eq. 5, as opposed to travel time weighted averaging for D_y in Eq. 4 is of interest. Particularly, three different solutions to the ADE, longitudinal routing, transverse routing, and the streamtube solution, all have different equations of reach unification. (Recall that for longitudinal routing it is a function of both travel time and velocity.) This result suggests that, at least in the case of ADE solutions with an exponential function, the variables inside the exponential (ignoring the distance/velocity square term and dispersion coefficient) indicate the type of averaging for reach unification.

3.2 Relating observed dispersion coefficient to reach characteristics

Reach unification is of significant interest to the inverse problem. That is, as opposed to knowing channel characteristics, calculating a dispersion coefficient, and making a prediction, instead using concentration data to obtain a dispersion coefficient and relating it to the channel characteristics. This challenge is one of the most widely investigated in dispersion, and numerous studies have attempted to derive predictors for the dispersion coefficient as a function of channel characteristics (e.g., Rutherford, 1994; Guymer, 2002; Boxall and Guymer, 2003; Zeng and Huai, 2014). This type of study is most often conducted for longitudinal dispersion and particularly in rivers that may vary over significant distances. How channel characteristics are distilled to a single value for comparison to experimentally derived dispersion coefficient values could significantly affect derived relationships.

To illustrate the impact of reach unification on dispersion coefficient predictors, the random channel characteristics have been used to re-derive the slope coefficient of the D_y relationship used to create the data (0.1300 in Eq. 15). The slope coefficient was best fit to the known D_y and the reach unified and length weighted channel characteristics with the y-intercept forced to be 0, i.e., 0 dispersion at 0 velocity. Fig. 4a-b compares D_y predicted using the new best-fit reach unified and length weighted slope coefficients to the actual dispersion coefficient.

The original slope coefficient of 0.1300 was recovered when using reach unified channel characteristics. Note that for reach unification, $\alpha = \sqrt{f/8}$ and $\alpha_i = \sqrt{f_i/8}$ in Eq. 14. Applying length weighted averaging gives a slope coefficient of 0.1047, a reduction of 23%, and shows significant scatter. While it follows the same trend, if only limited results were obtained, e.g., during fieldwork, a greater difference in the slope coefficient, and hence predictor, might be obtained. Sonnenwald et al (2023) show a similar result when comparing D_x over multiple sub-reaches averaged using different methods to the known D_x.

To further investigate averaging method, Fig. 4c-d show the results of other combinations of travel time and length weighted averaging. Fig. 4c combines travel time weighted averaging of U with length weighted averaging of f. Nearly the original slope coefficient, 0.1260, is obtained, showing the travel time weighted averaging of U to be critical. In contrast, Fig. 4d shows travel time weighted averaging of both U and f. While a similar slope of 0.1373 is again obtained, there is significantly more scatter. Both highlight the need for the appropriate averaging method to be applied to each variable.

The results shown here may in part explain one of the sources of error that has long plagued the mixing community when attempting to identify the dispersion coefficient predictors. Considering the need to, e.g., square a channel characteristic before applying Eq. 14 to obtain the reach unified characteristic, it is clear that there are implications for regression analysis when exponents are fit. Exponents should ideally be fit before averaging, although the low scatter of Fig. 4c suggests that in a first pass with exponents fit after reach unification, the correct functional form could still be identified.

4 Conclusions

The reach unification approach incorporates the characteristics (such as velocity, width, or dispersion coefficient) of each varying sub-reach into to the equivalent single reach values needed to make a direct downstream prediction when using simplified solutions to the Advection-Dispersion Equation (ADE). In this paper it is proposed, and shown, that reach unification is possible for the transverse ADE and is different than for the longitudinal ADE.

Reach unification for the transverse ADE consists of travel time weighted averaging of the transverse dispersion coefficient and longitudinal velocity, and length weighted averaging of other channel characteristics. This was confirmed using a finite difference model of the depth-averaged two-dimensional ADE to generate synthetic concentration data of a channel with multiple sub-reaches of varying ve-

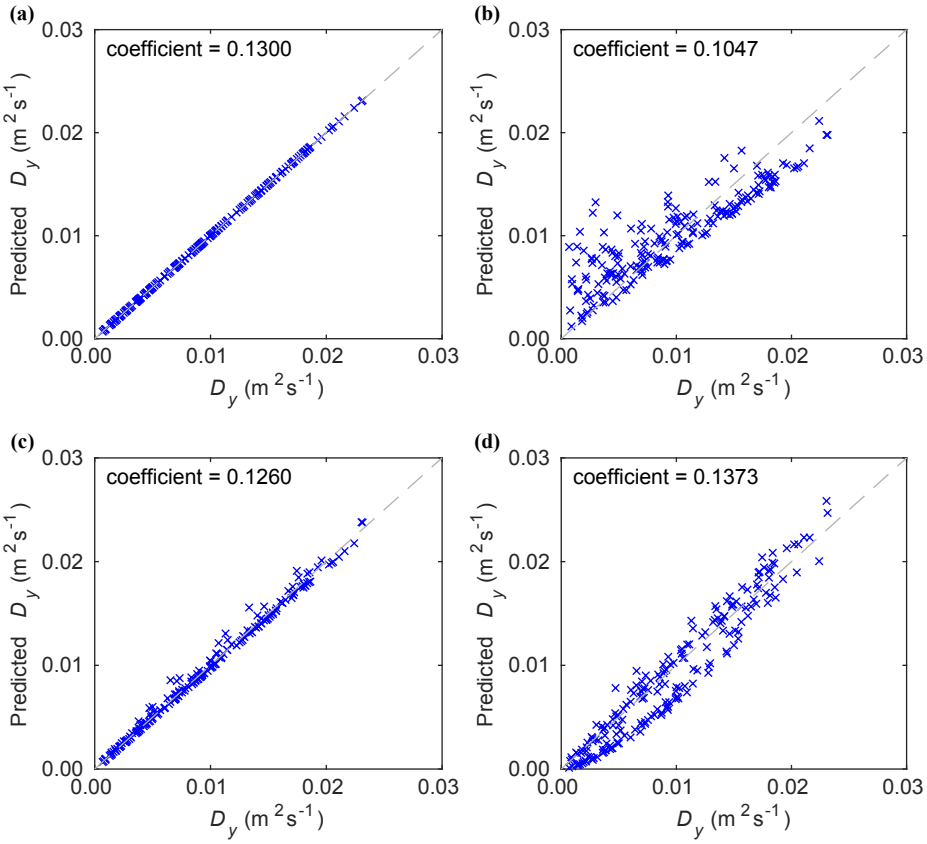

Fig. 4 Comparison of the known D_y and D_y predicted using **a** reach unified, **b** length weighted, **c** travel time weighted U and length weighted f, or **d** travel time weighted reach characteristics and, for each, the slope coefficient best-fit between the known D_y and those channel characteristics.

locity and roughness. These were predicted directly using reach unified dispersion coefficients with perfect agreement.

To account for changes in bathymetry when investigating transverse dispersion, reach unification can be combined with the streamtube model, in which case the reach unified transformed transverse dispersion coefficient is length weighted. The appropriate reach unification equations for the solution to the ADE of interest must be used, be that longitudinal, transverse, streamtube, or otherwise, and these are indicated by the variables in the solution.

Reach unification is of interest both when making predictions and when analysing experimental results, e.g., when linking observed dispersion to channel characteristics. The results show that if reach unification is applied, the original form of the dispersion coefficient relationship used when generating the synthetic data can be recovered. The use of incorrect averaging of channel characteristics, however, could result in an incorrect functional form or inaccurate model coefficients being identified. Special care should be taken when conducting regression analysis.

Acknowledgements This work was supported by the EPSRC (Grant No. EP/P012027/1). For the purposes of open access, the authors have applied a Creative Common Attribution (CC BY) license to any Author Accepted Manuscript version arising.

References

Boxall J, Guymer I (2003) Analysis and prediction of transverse mixing coefficients in natural channels. Journal of Hydraulic Engineering 129(2):129–139, DOI https://doi.org/10.1061/(ASCE)0733-9429(2003)129:2(129)

Fischer HB, List JE, Koh CR, Imberger J, Brooks NH (1979) Mixing in inland and coastal waters. Academic press

Guymer I (2002) A national database of travel time, dispersion and methodologies for the protection of river abstractions. R&D Technical Report P346, The Environment Agency

Kalinowska M, Rowiński P (2012) Uncertainty in computations of the spread of warm water in a river–lessons from environmental impact assessment case study. Hydrology and Earth System Sciences 16(11):4177–4190, DOI https://doi.org/10.5194/hess-16-4177-2012

Riechel M, Matzinger A, Pawlowsky-Reusing E, Sonnenberg H, Uldack M, Heinzmann B, Caradot N, von Seggern D, Rouault P (2016) Impacts of combined sewer overflows on a large urban river–understanding the effect of different management strategies. Water research 105:264–273, DOI https://doi.org/10.1016/j.watres.2016.08.017

Rutherford JC (1994) River mixing. Wiley, Chichester, England

Somlyódy L (1982) An approach to the study of transverse mixing in streams. Journal of Hydraulic Research 20(2):203–220, DOI https://doi.org/10.1080/00221688209499495

Sonnenwald F, Shuttleworth J, Bailey O, Williams M, Frankland J, Rhead B, Mark O, Wade MJ, Guymer I (2023) Quantifying mixing in sewer networks for source localisation. Journal of Environmental Engineering 149(5):04023,019, DOI https://doi.org/10.1061/JOEEDU.EEENG-7134

Stovin V, Sonnenwald F, Golzar M, Guymer I (2022) The impact of cylinder diameter distribution on longitudinal and transverse dispersion within random cylinder arrays. Water Resources Research 58(4):e2021WR030,396, DOI https://doi.org/10.1029/2021WR030396

Taylor GI (1954) The dispersion of matter in turbulent flow through a pipe. Proceedings of the Royal Society of London Series A Mathematical and Physical Sciences 223(1155):446–468, DOI https://doi.org/10.1098/rspa.1954.0130

West PO, Wallis SG, Sonnenwald FC, Hart JR, Stovin VR, Guymer I (2021) Modelling transverse solute mixing across a vegetation generated shear layer. Journal of Hydraulic Research 59(4):621–636, DOI https://doi.org/10.1080/00221686.2020.1818307

Yotsukura N, Cobb ED (1972) Transverse diffusion of solutes in natural streams. Tech. Rep. 582-C, Washington, DOI https://doi.org/10.3133/pp582C

Yotsukura N, Sayre WW (1976) Transverse mixing in natural channels. Water Resources Research 12(4):695–704, DOI https://doi.org/10.1029/WR012i004p00695

Young P, Jakeman A, McMurtrie R (1980) An instrumental variable method for model order identification. Automatica 16(3):281–294, DOI https://doi.org/10.1016/0005-1098(80)90037-0

Zeng Y, Huai W (2014) Estimation of longitudinal dispersion coefficient in rivers. Journal of hydro-environment research 8(1):2–8, DOI https://doi.org/10.1016/j.jher.2013.02.005